

Optimal charging of electric vehicle fleets: Minimizing battery degradation and grid congestion using Battery Storage Systems

David Geerts ^{*†}, Róbinson Medina [†], Wilfried van Sark ^{*}, Steven Wilkins ^{†,‡}

[†] Powertrains Department, TNO

^{*} Department of Geosciences, Utrecht University

[‡] Electrical Engineering department, Eindhoven University of Technology

Emails: [†] {Robinson.Medina, steven.wilkins}@tno.nl, ^{*} {d.c.geerts, w.g.j.h.m.vansark}@uu.nl

Abstract—The electrification of the transport industry is rapidly becoming a solution to mitigate the greenhouse emissions problem. However, this electrification faces multiple challenges related to higher operational cost and limited charging capacity. To cope with these challenges, within the European project URBANIZED, an optimization algorithm has been developed to determine charging schedules (i.e., charging current vs time) for electric vehicle fleets. The optimization algorithm exploits the benefits of adding a Battery Storage System (BSS) to the charging infrastructure. The algorithm minimizes the economical costs associated to charging a vehicle, such as battery degradation, grid connection and BSS costs, while taking into account vehicle-related and grid-related constraints. Simulation results show that charging the vehicle fleet as late as possible is the best way to reduce the total operation costs, due to the lower battery degradation. Likewise, the usage of a BSS allows to further increase the battery lifetime at an extra-cost of investing in a BSS system.

Keywords—Battery electric vehicles; Optimized charging scheme; Battery degradation; Grid congestion; Battery storage system.

I. INTRODUCTION

Greenhouse gas emission mitigation is one of the major challenges of the 21st century. The negative consequences of these emissions are already visible in the environment [1]. One way of reducing these emissions is by decreasing fossil-fuel usage. Such fuels are used in multiple sectors of the economy, with the transport sector alone accounting for 25% of its total usage via Internal Combustion Engines (ICEs) [2]. Reducing the fossil-fuel usage in the transport sector would significantly contribute towards solving the emissions problem.

Due to climate change, alternatives are being explored in the transport sector such as switching from ICEs to Battery Electric Vehicles (BEVs) [3]. During their life time, the emissions of BEVs are lower than those of ICEs [4]. They can even be close to zero when they are charged with electricity generated by renewable sources. However, the adoption of BEVs faces multiple challenges such as the relatively long charging time and a shorter driving range, when compared to ICE-based vehicles [5]. This implies that BEVs cannot drive long distances as time efficient as their ICEs-based counterparts. Adding to these challenges, the battery of BEVs continuously degrade over time, resulting in batteries with less capacity and further reducing the BEVs range [6]. Degradation is accelerated when stress factors are present in the battery cycle such as overcharge, depth of discharge or storing while fully charged [7]. Taking into account these stress factors is therefore crucial for the successful implementation of BEVs.

Another challenge related to the adoption of BEVs is the added load on the electrical grid resulting from charging such vehicles. Modern electrical grids were not designed to take into account the load peaks that charging BEVs fleets have on the total grid load. This leads to situations where grid operators might not be able to guarantee enough power for charging complete fleets of BEVs. For example, in The Netherlands, a large part of the electricity grid is already operating at nearly maximum capacity [8]. This implies that charging a few extra BEVs is feasible, but adding complete fleets might result in grid congestion. This challenge is more relevant for companies with (large) fleets of vehicles, such as bus operators or delivery companies. These companies would

require larger amounts of power (when compared to normal consumption) to charge their vehicles to continue with their normal operation [3]. Mitigating the grid impact of charging vehicles fleets is therefore crucial for the adoption of BEVs [9].

A potential solution for these challenges may be the use of Battery Storage Systems (BSSs). A BSS corresponds to a stationary battery used to support grid operation. A BSS is therefore charged when no or few BEVs are connected to the grid. It is discharged when a large amount of vehicles need charging. This BSS is placed close to the vehicles in a way that the connection between the vehicles and the BSS does not go through the grid. This reduces the BEVs impact on the grid at an extra cost of adding a BSS [10]. Another potential solution to these challenges is to dynamically decide when to charge the BEVs based on charging schemes (i.e., charging schedules). These schemes can be optimised to have not only the least impact on the grid, but also to reduce total charging cost. Combining these two solutions might lead to an optimized charging strategy with respect to the grid as well as the charging cost.

Charging a fleet of BEVs is a wide topic which has been studied from multiple angles. From the vehicle perspective, [11] showed in which cases a BSS can create revenue and how to optimize fleet charging. [12] showed what processes influence battery degradation and what the important factors are that accelerate degradation. From the fleet perspective, studies have been carried out on how to create charging schemes while minimizing some objective. For example, [13] showed what the optimised decentralized charging strategy would look like, while also taking into account network congestion. [14] shows the impact of uncontrolled charging of BEVs on the grid. They further elaborate on optimal charging strategies to mitigate such an impact. [15] developed an optimisation strategy for buses, where the desired routes and fleet charging were jointly determined. [16] developed an optimal charging algorithm taking into account electricity price. [17] focused on developing an algorithm for overnight charging of busses with respect to battery degradation and electricity price. None of this research considers the usage of a BSS and none take both grid capacity and battery ageing into account.

This paper presents an optimization algorithm that determines the charging schemes of BEVs, while including grid capacity restrictions and battery ageing in the BEVs

and BSS. The optimization algorithm uses a multilevel modelling strategy to capture the dynamics of the system: from battery models to fleet-level cost models. Multiple cost functions are minimized and compared aimed at reducing battery ageing and CO_2 emissions related to the electricity production, while optimizing grid connection size.

This paper is divided as follows. Section II introduces the used modelling strategy for vehicle batteries. Section III defines the mathematical aspects of the optimization algorithm. Section IV discusses the result of applying the optimization algorithm to a case study. Section V closes the paper with conclusions.

II. BATTERY MODELLING STRATEGY

To optimize the charging schedule of a fleet of BEVs, multiple models are required to capture the dynamics in the vehicle battery and battery degradation. The following subsections present the used models.

A. Battery Model

The second order Equivalent Circuit Model (ECM) shown in Fig. 1 is used to model a battery cell [18]. Using this ECM, the following model is derived:

$$\begin{aligned} V_{cell} &= V_{OCV} + I_{cell}R + V_1 + V_2 \\ \frac{dV_1}{dt} &= \frac{I_{cell}}{C_1} - \frac{V_1}{R_1C_1} \\ \frac{dV_2}{dt} &= \frac{I_{cell}}{C_2} - \frac{V_2}{R_2C_2}, \end{aligned} \quad (1)$$

where V_{cell} denotes the terminal cell voltage, V_{OCV} is the open circuit voltage, I_{cell} cell current, R , R_1 , and R_2 are resistances, V_1 and V_2 are polarization voltages over the RC tanks, and C_1 and C_2 are capacitors. All magnitudes in this paper are expressed in SI units unless noted otherwise. The model parameters C_1 , C_2 , R_1 , R_2 , R and V_{OCV} are dependent on the current direction (i.e., charging or discharging), cell temperature, and State of Charge (SOC). An example of these parameters can be found in Fig. 2. The current and voltage at pack level is computed by scaling up the cell current and voltage, i.e.,

$$\begin{aligned} I &= I_{cell}n_p \\ V &= V_{cell}n_s, \end{aligned} \quad (2)$$

where I is the pack current, n_p is the number of parallel cells in the pack, V is the pack voltage, and n_s is

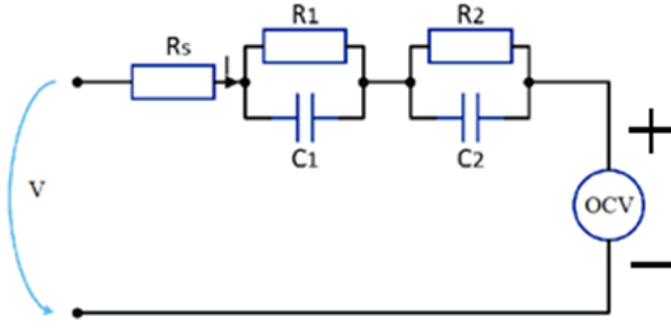


Fig. 1: Overview second order equivalent circuit model, extracted from [18]

the number of cells in series in the pack. The SOC is calculated with coulomb counting

$$Z_{k+1} = Z_k + \frac{I_k dk}{3600 C_{orig}}, \quad (3)$$

where Z is the SOC, C_{orig} is the capacity of the whole battery in Ah, the constant 3600 is used to convert seconds to hours, k is the discrete-time index, and dk the length of one time step in hours. This time step is assumed to be 0.25 hours. Such a value saves on computational time, while maintaining the accuracy needed for the optimization.

Based on the battery model presented in this subsection, a degradation model and thermal model for batteries are introduced in the next subsections.

B. Degradation of batteries

Although multiple processes cause degradation in batteries, these can be grouped in two categories: calendar ageing and cyclic ageing. The first happens over time, whether the battery is used or not. This type of ageing is mainly caused by an irreversible and unintended side reactions that slowly consumes the lithium in the battery [19]. Cyclic ageing happens only when the battery is used and is mainly caused by forming an unintended layer on the anode, which hinders or prevents the anode from releasing electrons, therefore reducing the capacity of the battery [20]. To capture these degradation processes, [19] proposed an empirical model which takes into account SOC, current, voltage, battery temperature, and time to calculate the corresponding degradation of a cell. Such a degradation is expressed in terms of capacity loss and resistance increase. For this research only the loss of capacitance is considered as the optimizer is designed

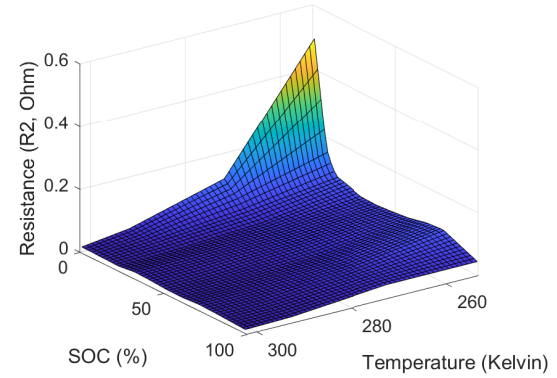
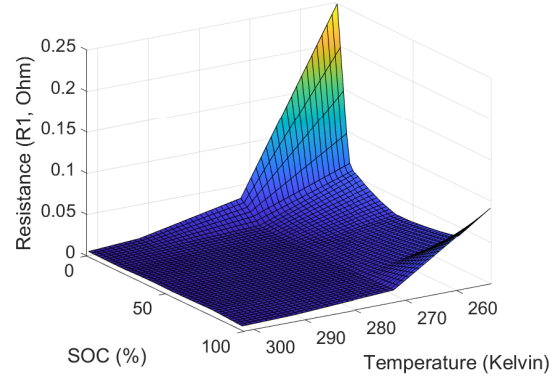
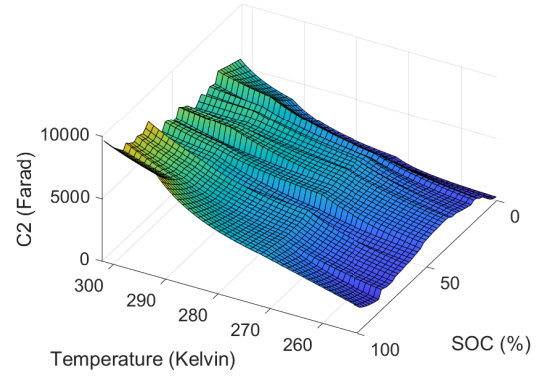
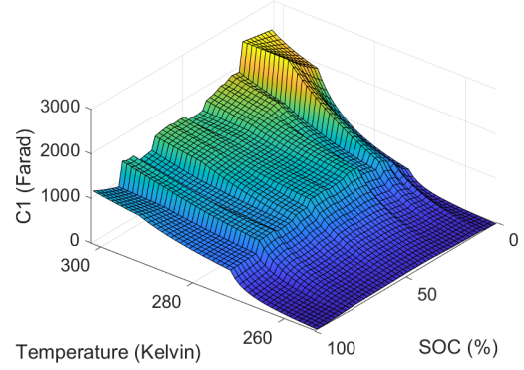


Fig. 2: Example of parameters for the ECM under charging conditions

to minimize capacity loss. Including resistance increase remains an interesting research topic.

The calendar loss is defined by [19] as

$$C_{after}^{cal} = 1 - (7.543\bar{V}_{cell} - 23.75) \times 10^6 \exp\left\{-\frac{6976}{\bar{T}_{cell}} T^{0.75}\right\}, \quad (4)$$

with \bar{V}_{cell} the average voltage over one cell, \bar{T}_{cell} the average cell temperature in Kelvin, and T the time in days. C_{after}^{cal} is the new capacity after T days if only the calendar aging is taken into account, which ranges from 0 to 1.

Cycling aging is defined as

$$C_{after}^{cyc} = 1 - (7.348 \times 10^{-3}(V_{RMS} - 3.67)^2 + 7.6 \times 10^{-4} + 4.08 \times 10^{-3}(1 - Z))\sqrt{Q}, \quad (5)$$

where

$$Q = (1 - Z)C_{origin}T_{cycles}. \quad (6)$$

Here V_{RMS} is the root mean square of the cell terminal voltage, $1 - Z$ is the depth of discharge, Q is the cell charge throughput of one cycle in Ah, and T_{cycles} is the number of cycles. C_{after}^{cyc} is the new capacity after T_{cycles} cycles if only the cyclic aging is taken into account. The updated capacity is obtained using

$$C_{new} = C_{orig}(-1 + C_{after}^{cal} + C_{after}^{cyc}), \quad (7)$$

where C_{new} is the new capacity after a cycle has been applied.

The updated capacity, computed with Eq. 7, is used in the optimization process to calculate the cost of degradation (see Section III). Note that this updated capacity requires average cell temperature as one of its inputs. The computation of this temperature is explained in the next subsection.

C. Thermal model

A thermal model at cell level is used to compute the cell temperature. The thermal model considers the addition of four heat flows [21], [22], i.e.,

$$C_{heat,cell} * m_{cell} \frac{dT_{cell}}{dt} = \dot{Q}_s + \dot{Q}_O - \dot{Q}_B + \dot{Q}_{cool}, \quad (8)$$

where \dot{Q}_s is the reversible reaction heat, \dot{Q}_O is the overpotential heat, \dot{Q}_B is the heat transferred to the environment, and \dot{Q}_{cool} is the heat added by a cooling system. All heat flows are expressed in watts. $C_{heat,cell}$ is the heat capacity of one cell and m_{cell} is the mass of

one cell. The multiple heat flows are further described as:

$$\begin{aligned} \dot{Q}_s &= T_{cell} I_{cell} \frac{\partial V_{OCV}}{\partial T_{cell}} \\ \dot{Q}_O &= RI_{cell}^2 + \frac{V_1^2}{R_1} + \frac{V_2^2}{R_2} \\ \dot{Q}_B &= R_{th}(T_{cell} - T_{amb}), \end{aligned} \quad (9)$$

where $\partial V_{OCV}/\partial T_{cell}$ is the partial derivative of the open circuit voltage with respect to the cell temperature. This parameter is obtained via experiments and depends on the SOC. R_{th} is the thermal resistance between the battery surface and the environment. T_{amb} is the ambient temperature. Note that \dot{Q}_{cool} depends on the cooling capacity of the thermal system and the battery geometry, therefore a general definition is not included in Eq. 9.

Based on the modelling framework presented in these subsections, an optimization algorithm is defined in the next section.

III. OPTIMIZATION OBJECTIVE

This section details the cost function and the constraints used in the optimization algorithm.

A. Cost function definition

The optimization objective minimizes some cost \mathbb{C}_{tot} , which consists of four components: a degradation-related cost (\mathbb{C}_{degr}), CO₂-related costs (\mathbb{C}_{CO_2}), grid-connection costs (\mathbb{C}_{grid}), and BSS-related cost (\mathbb{C}_{BSS}). This is captured by the following optimization problem:

$$\begin{aligned} \min_{\mathbb{I}} \quad & \mathbb{C}_{tot} \\ \text{s.t.} \quad & \text{Eq. 17, Eq. 18} \\ & \text{Eq. 19, Eq. 20,} \end{aligned} \quad (10)$$

where \mathbb{I} is a set of current profiles that charges each vehicle in the fleet, further defined by

$$\mathbb{I} = \{I_{n,k} \mid n = 1, \dots, N_{fleet} \wedge k = 1, \dots, T_{charge}\},$$

where N_{fleet} is the number of vehicles in the fleet and T_{charge} is the number of steps in which the total charging time is divided. Note that T_{charge} is a design choice: a large number of steps results in a more detailed current profile at an extra cost of computational effort. $I_{n,k}$ is the charging current during time slot t of vehicle n . The definition of $I_{n,k}$ implies that the current is discrete during the duration of each time slot dk . Furthermore, the total cost is defined as

$$\mathbb{C}_{tot} = \mathbb{C}_{degr} + \mathbb{C}_{CO_2} + \mathbb{C}_{grid} + \mathbb{C}_{BSS}. \quad (11)$$

Each cost is expressed in euro. This function excludes the price for electricity. The underlying assumption the electricity price is fixed throughout the day.

For the degradation-related costs, it is assumed that the end of life of a battery occurs when the battery capacity is 80% or lower. The battery is assumed to have no second-life value, which implies that its value is zero when the capacity reaches the end of life. This is considered common practice among researchers [23]. The degradation-related costs are given by

$$C_{degr} = \frac{C_{orig} - C_{new}(T_{sim}, I)}{0.2C_{orig}} C_{batt}, \quad (12)$$

where C_{new} is the in resulting capacity after the optimal charging cycle has been applied. C_{new} is calculated using Section II-B. Note that the pack current I influences the amount of degradation as shown in Section II. Moreover, the degradation is only computed for the charging period T_{sim} . The constant 0.2 takes into account the end of life spam (i.e., 80% of original capacity). C_{batt} is the initial battery price in euros.

The costs related to CO₂ generation are calculated using

$$C_{CO_2} = \sum_{k=1}^{T_{charge}} \left(\sum_{n=1}^{N_{fleet}} P_{n,k} \times E_{CO_2,grid} dk \right) \times C_{CO_2,gram} T_{sim}, \quad (13)$$

with

$$P_{n,k} = V_{n,k} I_{n,k}. \quad (14)$$

Here, $P_{n,k}$ is the power demand for charging at time step t and vehicle n . $E_{CO_2,grid}$ is the CO₂ emissions of the electricity in the grid at the time step k in grams of CO₂ per kWh. The CO₂ emissions of the grid were calculated using data from [24]. An example of the CO₂ emissions is shown in Fig. 3. Note that $k = 0$ corresponds to the starting time of 20:00. $C_{CO_2,gram}$ are the costs related to each gram of produced CO₂. This is based on the average of the European Emission Trading System (EU ETS), which assigns a price to CO₂ generation. $V_{n,k}$ is calculated using Eq. 2. T_{sim} is the length of the simulation in days.

The cost related to the grid connection are based on data from [25]. The costs for the grid connection are formulated as

$$C_{grid} = \frac{C_{fix} + C_{var} S_{connection}}{365.25} \times T_{sim}. \quad (15)$$

The costs consist of a fixed (C_{fix}) and a variable part (C_{var}). Both of these costs dependent on the connection

TABLE I: Example of operational costs per grid connection size in The Netherlands [25]

Grid connection size (kW)	Fixed cost (€/year)	Variable cost (€/kW*year)
0 - 175	208	44.63
176 - 1750	812	34.70
1751 - 3000	2239	34.70
3001 - 6000	2351	29.83

size ($S_{connection}$). An example of such costs can be found in Table I, which shows the prices in The Netherlands for companies. Cost of connections larger than 6000 kW are not given by the grid operator, since they are highly dependent on the situation. These situations are therefore not be considered in this paper [25]. The constant 365.25 converts the cost from year to day.

To compute the cost of the BSS, it is assumed that the BSS has a life time of 4 years when used every day [26]. Therefore the cost is described as

$$C_{BSS} = \frac{C_{BSS} \rho_{BSS}}{\Gamma} \times T_{sim}. \quad (16)$$

The discharged energy of the BSS (C_{BSS}) is in kWh. ρ_{BSS} is the BSS price which can be found in Table II. Based on [26], the cost of a BSS in 2022 is 100 euros per kWh. Γ is the battery lifetime in days.

B. Constraints formulation

The objective of the optimization is to minimize the total cost function as described in Eq. 10. The constraints are the following:

$$\sum_{n=1}^{N_{fleet}} P_{n,k} \leq P_{grid,k} + P_{BSS,k} \quad (17)$$

$$\text{for all } k \in \{1, \dots, T_{charge}\},$$

$$\sum_{k=1}^{T_{charge}} P_{BSS,k} dk \leq C_{BSS}, \quad (18)$$

$$0.97 \leq Z_{n,T_{charge}} \leq 0.99 \quad (19)$$

$$\text{for all } n \in \{1, \dots, N_{fleet}\},$$

$$I_{n,k} \geq 0 \text{ for all } n, k. \quad (20)$$

Here, $P_{grid,k}$ and $P_{BSS,k}$ are the power delivered by the grid and BSS respectively.

Each one of the constraints shown above have a different purpose. For example, Eq. 17 makes sure that the power used by all the vehicles never exceeds the

TABLE II: Example of model parameters values

Parameter	Value	Unit
Ambient temperature	283	K
Battery price EV new	16,000	€
BSS price	100	€/kWh
Battery Capacity EV	142.5	Ah
Specific heat capacity one cell	880	J/(kg*K)
Thermal resistance between cell and ambient	2.94	W/K
CO ₂ costs	80	€/tonne CO ₂
Observed month for CO ₂ cost	November	-
Cells in parallel	50	-
Cells in series	96	-

amount that the grid and the BSS can deliver at a time instant k . Eq. 18 takes into account that the total power that is drawn from the BSS cannot exceed the stored energy of the BSS (C_{BSS}). The BSS is assumed to be fully charged at $k = 0$ and can be fully discharged at T_{charge} . Eq. 19 makes sure that the battery of each vehicle is charged to at least 97% before the end of the charging period and not more than 99%. Eq. 20 is the lower bound, which prevents the current from being negative.

This section presented the details of the optimization algorithm used to schedule the charging schedule of a fleet of electric vehicles. The optimization is applied and analysed in a case study in the next section.

IV. SIMULATION RESULTS AND DISCUSSION

This section illustrates the applicability of the optimization algorithm, based on a realistic case study.

A. Case study

To show the benefits of the optimization algorithm, a case study was created, which gives insights in how the algorithm works. The case study is based on lightweight electric freight trucks, used for last-mile deliveries. The BEV weighs a maximum of 3500 kilogram including payload. This weight makes these vehicles an attractive solution for a fleet operator, because no truck driver license is required.

The BEVs are used for deliveries throughout the day. At the end of the day, all vehicles are brought back to the same depot and can be charged overnight from 20:00 till 8:00. They can be charged with different currents, which is decided by a central coordinator, i.e., the optimization algorithm of Section III. Fleet sizes of 20, 40, and 60 vehicles are considered for simulation purposes. For the CO₂ emissions, the month of November is considered as

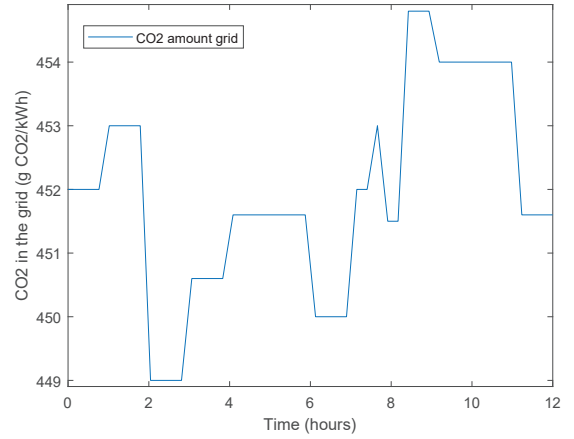


Fig. 3: Amount of CO₂ in the grid during the month of November in The Netherlands Fig. 3

Fig. 3 shows. In the figure, $Time = 0$ corresponds with the start time of charging, namely 20:00 hours.

The batteries are assumed to be Li(NiMnCo)O₂ 18650 lithium-ion batteries. The batteries are modeled as explained in Section II. The model parameters of Fig. 2 are used in the simulation. All vehicles are assumed to have a starting SOC of 30%. To easily analyse the results, all vehicles are assumed to have the same model parameters. However, notice that the methodology presented in this paper supports different parameters sets. An overview of the model parameters is shown in Table II. The BEVs do not have active cooling/heating of their batteries (i.e., $\dot{Q}_{cool} = 0$). However, in case of vehicles with this system, this heat flow could be added as explained in [22].

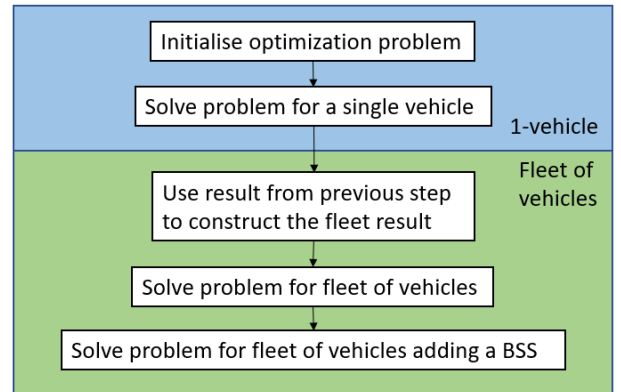


Fig. 4: The optimization flowchart

Using the steps presented in Section III, the cost function and constraints are formulated. The optimal

problem was solved using Matlab, which runs an interior-point algorithm. A flowchart of the optimization can be found in Fig. 4. To speed up the optimization, the solution of the single-vehicle result was used as input (i.e., initial solution) for the fleet-level problem.

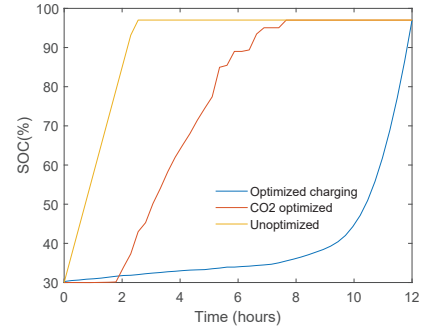
B. Single-vehicle result

To intuitively show the results of the optimization strategy, the problem is solved first for a fleet with a single vehicle. Three scenarios are considered, where the grid cost were neglected as they are constant for one vehicle, i.e., $C_{grid} = 0$. For the same reason, no BSS is included, i.e., $C_{BSS} = 0$. The three scenarios are:

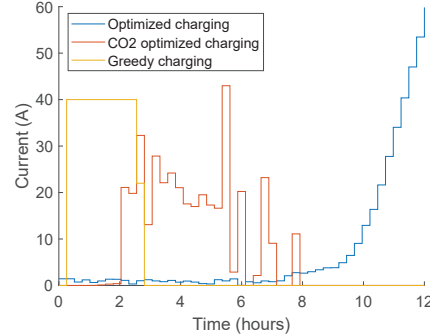
- *Greedy charging*: No optimization is applied. This implies that the vehicles are charged at the moment they are connected with a charging current high enough to charge the pack in approximately 3 hours.
- *Optimized charging*: A charging schedule is derived solving the optimization objective presented in Eq. 10.
- *Optimized charging for CO₂ emissions minimization*: The optimization presented in Eq. 10 is solved only taking into account the CO₂ component, to generate a charging schedule that emits the least amount of CO₂ emissions, i.e., $C_{tot} = C_{CO_2}$.

The resulting SOC and charging profile per scenario can be seen in Figs. 5a and 5b, respectively. In both figures, $time = 0$ corresponds to the starting time of 20:00, which is moment when the BEVs are connected. The greedy charging scenario charges the vehicle as soon as it arrives. The optimized charging charges as late as possible. This is because charging late reduces the average and RMS voltage in Equations (4) and (5). Reducing these voltages leads to less degradation. Likewise, the optimized charging scheme shows higher charging currents than the greedy scenario, as this would generate lower degradation. Notice that the greedy scenario was only created for reference, therefore it does not apply the highest possible charging current.

The CO₂ optimized scenario charges when the CO₂ concentration is the lowest on the grid, i.e., between 2:00 and 5:00, as can be seen from Fig. 3. In that time frame, the emissions are low, because the total share of wind and nuclear energy becomes relatively higher, as fossil



(a) SOC comparison



(b) Current profile comparison

Fig. 5: Single-vehicle simulation

fuel-based energy sources are turned down since less electricity is required in the grid.

Fig. 6 shows the cost comparison of the single-vehicle result. There it can be seen that the greedy scenario is the worst cost wise, with the degradation costing €7.92 (71%) more than the optimized scenario. The CO₂ optimized scenario shows the little relevance of the CO₂ cost. This scenario has the lowest CO₂ cost which is only €0.05 (3%) lower than the optimized charging scheme, while the degradation costs is €4.82 (43%) higher. This is because the price of CO₂ is relatively low, and the variation of CO₂ in the grid is minor, which results in only around 40 g CO₂/kWh saved in the simulation. This does not compensate for the increased degradation. This optimization becomes more relevant in grids with significant variations of CO₂ emissions during the day.

C. Fleet results

In the case of fleet charging, fleets with sizes of 20, 40, and 60 vehicles are analyzed. A comparison is made for each fleet size in three different scenarios, namely:

- *Unconstrained optimized charging*: A charging

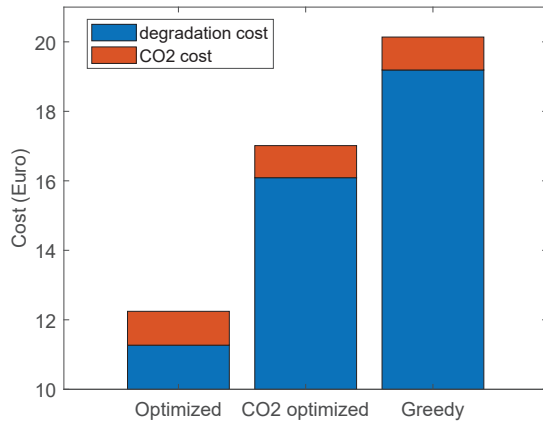


Fig. 6: Cost comparison single vehicle

schedule is obtained by solving the optimization problem of Eq. 10 without taking into account the maximum grid connection constraint (i.e., the grid capacity is unlimited) in Eq. 17 and thus ignoring the constraint in Eq. 18 as well.

- *Constrained optimized charging without BSS:* A charging schedule is derived solving Eq. 10 with a maximum grid capacity of 175 kW. This power is chosen as this is the highest possible connection within the lowest price range, as described in Table I. No BSS is present in the system.
- *Constrained optimized charging with BSS:* The same scenario as above including a 30, 100, 100 kWh BSS for fleet sizes of 20, 40, 60, respectively.

Each one of these scenarios are compared in terms of power consumption, total resulting cost, and influence of the BSS size.

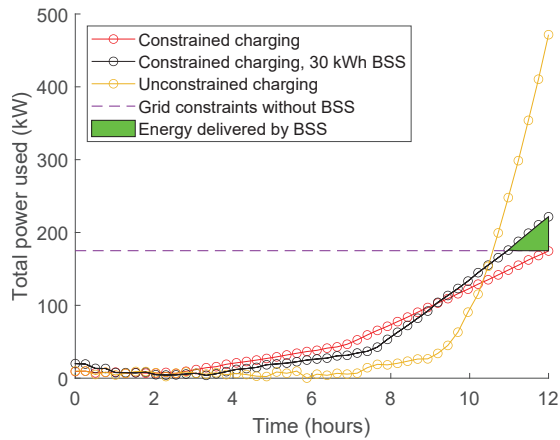
1) *Power comparison:* The resulting total power that the fleet uses each time step can be found in Fig. 7. The dashed horizontal line shows the grid restriction. The unconstrained optimal charging profile charges later than the constrained one without a BSS, as the constrained one has to ensure to stay below the grid limitation, while ensuring that every car is fully charged. Note that the unconstrained scenario, the charging power exceeds the grid limit (as it is designed to be). The resulting power profile is comparable to the optimized charging scheme in Fig. 5b. For the BSS scenario, the area above the dotted line is the energy provided by the BSS. This allows the optimal charging to go above the grid constraint.

In the constrained scenario without a BSS with a fleet size of 60 BEVs, the constraint which forces each vehicle to be fully charged (Eq. 19) cannot be met due to insufficient energy available in the grid during the available charging time. For the same fleet with a BSS of 100 kWh, this constraint is (barely) met and a peak of 370 kW is observed, which is twice as high as the grid connection. This might become unrealistic and needs further analysis from a practical point of view and is therefore left out of further analysis.

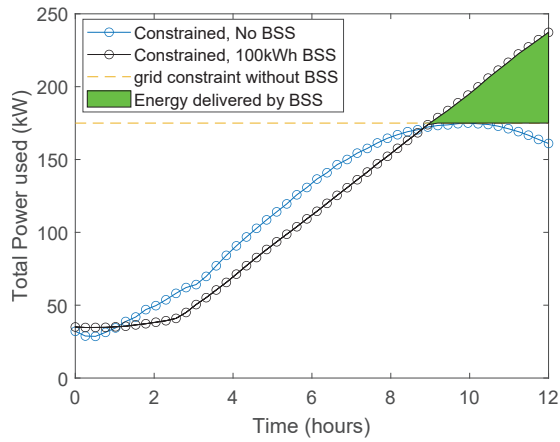
2) *Cost comparison:* In Fig. 8, a cost comparison (i.e., the evaluation of Eq. 11) can be found for each fleet size and aforementioned scenarios. For the 20 and 40 vehicles fleet, the scenario with the BSS shows the least total cost, saving 7% and 12.4% for a fleet size of 20 and 40, respectively, compared to the unconstrained scenario. Likewise, for both fleet sizes the constrained scenario without BSS is more cost effective than the unconstrained scenario. The addition of a BSS is cost effective by a 1% margin compared to the constrained scenario. The differences in CO₂ cost for each scenario are almost negligible. Note that the unconstrained case shows the least degradation cost, because this strategy allows to charge the battery the last.

Fig. 8c shows the costs results with a 60 vehicle fleet. Note that the constrained case without BSS is left out due to its infeasibility. The figure shows that at this fleet size, the constrained scenario with BSS results in higher costs. The costs related to degradation are higher than the associated cost of the grid connection. Therefore a bigger connection is more cost effective.

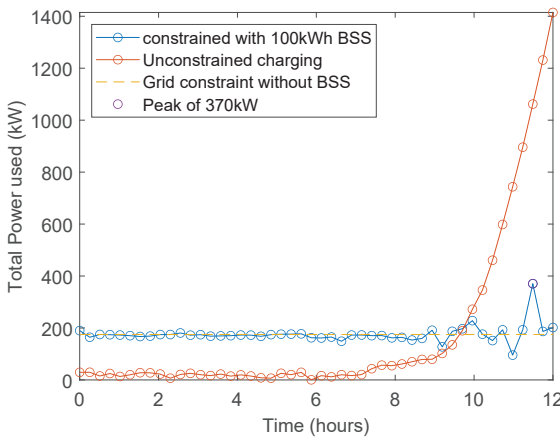
3) *BSS size comparison:* The influence of multiple BSSs sizes in the total cost is shown in Fig. 9. The fleet size of 60 vehicles is not shown for the practical reasons discussed earlier. It can be seen that there is an optimal size for the BSS and this is dependent on fleet size. For a fleet of 20 vehicles this optimum lies between 10 and 30 kWh, but the profit margin is less than 1%. For a fleet size of 40 vehicles, the optimal BSS size lies around 300 kWh. This margin is larger, namely 2.8%. With larger fleet sizes the addition of a BSS therefore becomes more cost effective. The more constrained the grid becomes the more cost effective the BSS can be, due to the fact that the BSS provides more freedom to the optimizer, which results in lower battery degradation.



(a) 20 vehicle fleet

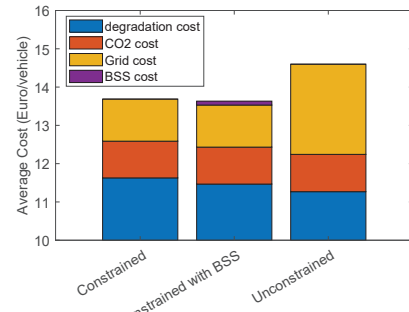


(b) 40 vehicle fleet

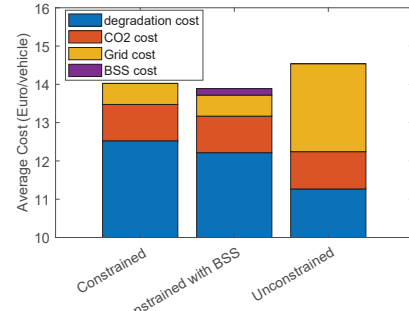


(c) 60 vehicle fleet

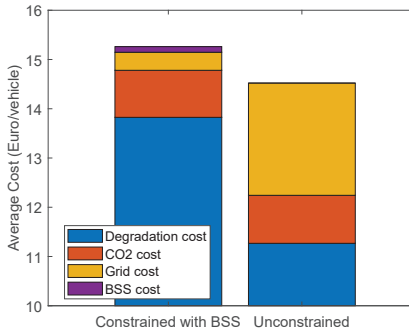
Fig. 7: Total power required for charging each fleet size



(a) 20 vehicle fleet



(b) 40 vehicle fleet



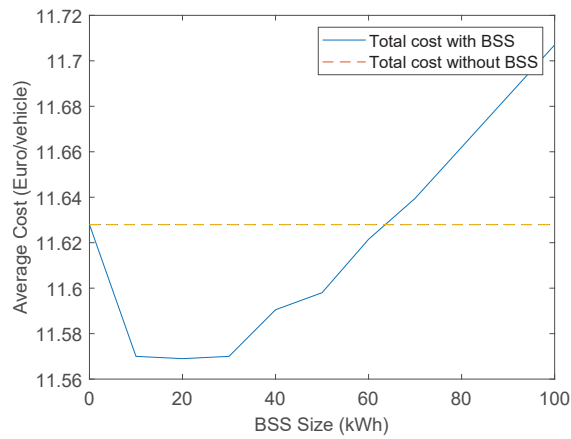
(c) 60 vehicle fleet

Fig. 8: Cost comparison for charging each fleet size

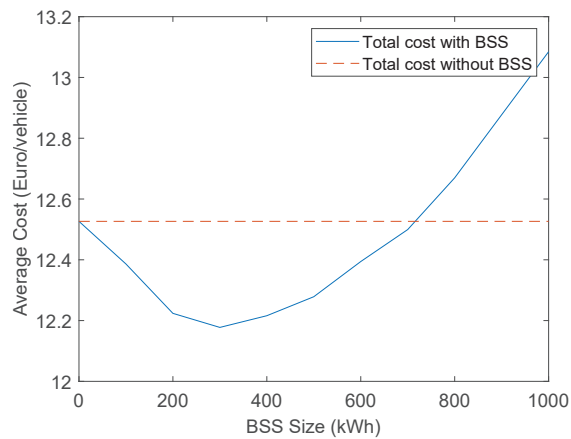
V. CONCLUSION

This paper showed an optimal charging strategy for a fleet of Battery Electric Vehicles (BEVs) using a Battery Storage System (BSS). The optimal charging strategy is based on a modelling strategy that captures the battery dynamics and battery degradation. The optimal charging strategy minimizes the combined effects of the degradation cost of the batteries in the BEV, the cost related to CO₂ generation, the cost of the BSS, and the grid connection costs.

To show the applicability of the optimal charging



(a) 20 vehicle fleet



(b) 40 vehicle fleet

Fig. 9: Battery cost for different battery size

strategy, a case study is presented where multiple fleet sizes and BSS are compared. For comparison purposes, a “greedy” charging strategy (i.e., charging as soon as the vehicle arrives to the depot) is applied to the case study. This case study shows that, first, the optimization algorithm provides a charging strategy that results in lower total costs in all compared scenarios. For example, in a single-vehicle charging scheme, the degradation costs are 71% higher when greedy charging is used than with an optimized charging scheme. This was achieved by charging the vehicles as late as possible, as it corresponds in the least amount of battery ageing. Second, using an optimal charging algorithm can further reduce the total costs and degradation costs by using a BSS. For example, the total cost of charging a fleet of 20 and 40 vehicles is reduced by 1% and 2.8%, respectively, while using a BSS. However, this result cannot be generalized

to all cases as it depends on multiple factors such as grid connection and energy requirements. Third, the grid connection cost and battery degradation costs are the dominant factors in the total cost of charging a fleet of BEV. The optimal charging strategy is shown to reduce mostly these costs. Likewise, the effect of CO₂ costs are marginal and could not be significantly reduced by the optimization algorithm. This is due the low variations of CO₂ emissions from the grid through the day and the relatively low cost of these emissions.

ACKNOWLEDGMENT

This research has received funding from the European Union’s Horizon 2020 research and innovation programme under grant agreement No 101006943, under the title of URBANIZED (<https://urbanized.eu/>). For the purpose of open access, the author has applied a CC BY-ND public copyright licence to any Author Accepted Manuscript version arising from this submission.

REFERENCES

- [1] V. Masson-Delmotte *et al.*, “Summary for Policymakers. In: Climate Change 2021: The Physical Science Basis. Contribution of Working Group I to the Sixth Assessment Report of the Intergovernmental Panel on Climate Change,” IPCC, Tech. Rep., 2021.
- [2] Z. Zhongming *et al.*, “Companion to the Inventory of Support Measures for Fossil Fuels 2021,” OECD, Tech. Rep., 2021.
- [3] I. Sotnyk *et al.*, “Development of the US electric car market: Macroeconomic determinants and forecasts,” *Polityka Energetyczna*, vol. 23, 2020.
- [4] W. J. Smith, “Can EV (electric vehicles) address Ireland’s CO₂ emissions from transport?” *Energy*, vol. 35, no. 12, pp. 4514–4521, 2010.
- [5] S. Orcioni and M. Conti, “EV Smart Charging with Advance Reservation Extension to the OCPP Standard,” *Energies*, vol. 13, no. 12, p. 3263, 2020.
- [6] B. Xu *et al.*, “Modeling of lithium-ion battery degradation for cell life assessment,” *IEEE Trans. on Smart Grid*, vol. 9, no. 2, pp. 1131–1140, 2016.
- [7] J. Guo *et al.*, “Impact analysis of V2G services on EV battery degradation-a review,” *2019 IEEE Milan PowerTech*, pp. 1–6, 2019.
- [8] Liander, “Beschikbaarheid capaciteit per gebied (Available capacity per region),” <https://www.liander.nl/transportschaarste/beschikbaarheid-capaciteit>, accessed: 2022-04-27.
- [9] S. M. Hosseini *et al.*, “Distributed control of electric vehicle fleets considering grid congestion and battery degradation,” *Internet Technology Letters*, vol. 3, no. 3, p. e161, 2020.
- [10] H. Das *et al.*, “Electric vehicles standards, charging infrastructure, and impact on grid integration: A technological review,” *Renewable and Sustainable Energy Reviews*, vol. 120, p. 109618, 2020.

- [11] M. Klausen, M. Resch, and J. Bühler, "Analysis of a potential single and combined business model for stationary battery storage systems," *Energy Procedia*, vol. 99, pp. 321–331, 2016.
- [12] T. Waldmann *et al.*, "Temperature dependent ageing mechanisms in Lithium-ion batteries—A Post-Mortem study," *Journal of Power Sources*, vol. 262, pp. 129–135, 2014.
- [13] R. Carli and M. Dotoli, "A distributed control algorithm for optimal charging of electric vehicle fleets with congestion management," *IFAC-PapersOnLine*, vol. 51, no. 9, pp. 373–378, 2018.
- [14] J. A. P. Lopes, F. J. Soares, and P. M. R. Almeida, "Integration of electric vehicles in the electric power system," *Proceedings of the IEEE*, vol. 99, no. 1, pp. 168–183, 2010.
- [15] M. Rogge *et al.*, "Electric bus fleet size and mix problem with optimization of charging infrastructure," *Applied Energy*, vol. 211, pp. 282–295, 2018.
- [16] A. Houbbadi *et al.*, "Multi-objective optimisation of the management of electric bus fleet charging," in *2017 IEEE Vehicle Power and Propulsion Conference (VPPC)*. IEEE, 2017, pp. 1–6.
- [17] —, "Optimal scheduling to manage an electric bus fleet overnight charging," *Energies*, vol. 12, no. 14, p. 2727, 2019.
- [18] B. Huang *et al.*, "A novel electro-thermal model of lithium-ion batteries using power as the input," *Electronics*, vol. 10, no. 22, p. 2753, 2021.
- [19] J. Schmalstieg *et al.*, "A holistic aging model for li (nīmncō) o₂ based 18650 lithium-ion batteries," *Journal of Power Sources*, vol. 257, pp. 325–334, 2014.
- [20] E. Redondo-Iglesias, P. Venet, and S. Pelissier, "Calendar and cycling ageing combination of batteries in electric vehicles," *Microelectronics Reliability*, vol. 88, pp. 1212–1215, 2018.
- [21] C. Zhang *et al.*, "Charging optimization in lithium-ion batteries based on temperature rise and charge time," *Applied energy*, vol. 194, pp. 569–577, 2017.
- [22] K. Onda *et al.*, "Experimental study on heat generation behavior of small lithium-ion secondary batteries," *Journal of the Electrochemical Society*, vol. 150, no. 3, p. A285, 2003.
- [23] M. H. S. M. Haram *et al.*, "Feasibility of utilising second life ev batteries: Applications, lifespan, economics, environmental impact, assessment, and challenges," *Alexandria Engineering Journal*, vol. 60, no. 5, pp. 4517–4536, 2021.
- [24] ElectricityMap, "Live 24/7 co2 emissions of electricity consumption." 2022. [Online]. Available: <https://app.electricitymap.org/map>
- [25] Enexis, "Grootzakelijke aansluiting gas en elektriciteit: Enexis netbeheer," 2022. [Online]. Available: <https://www.enexis.nl/zakelijk/aansluitingen>
- [26] E. technology and innovation platform, "Strategic research agenda for batteries 2020 - european commission," 2020. [Online]. Available: https://ec.europa.eu/energy/sites/ener/files/documents/batteries_europe_strategic_research_agenda_december_2020__1.pdf